Article

Modelling the rising tails of galaxy rotation curves

Fan Zhang [1,†,‡]

1   Gravitational Wave and Cosmology Laboratory, Department of Astronomy, Beijing Normal University, Beijing 100875, China; fnzhang@bnu.edu.cn
2   Department of Physics and Astronomy, West Virginia University, PO Box 6315, Morgantown, WV 26506, USA; fnzhang@mail.wvu.edu

Abstract: It is well known but under-appreciated in astrophysical applications, that it is possible for gravity to take on a life of its own in the form of Weyl-curvature-only metrics (note we are referring to the Weyl-only solutions of ordinary General Relativity, we are not considering Weyl conformal gravity or any other modified gravity theories), as numerous examples demonstrate the existence of gravitational fields not being sourced by any matter. In the weak field limit, such autonomous gravitational contents of our universe manifest as solutions to the homogeneous Poisson's equation. In this note, we tentatively explore the possibility that they may perhaps account for some phenomenologies commonly attributed to dark matter. Specifically, we show that a very simple solution of this kind exists that can be utilized to describe the rising tails seen in many galaxy rotation curves, which had been difficult to reconcile within the cold dark matter or modified Newtonian dynamics frameworks. This solution may also help explain the universal ~ 1Gyr rotation periods of galaxies in the local universe.

Keywords: dark matter; galaxies; gravitation; rotation curves; galaxy rotation period

1. Introduction

A confirmation of the nature of dark matter (DM) remains elusive. Weakly Interacting Massive Particles are recently running up against strong constraints set by the null results of direct [3,5,18] and indirect [2] detection experiments. Astrophysical observations have also ruled out the original version of axions proposed to solve the strong CP problem [23,24], and searches for its "invisible" reincarnations have also become severely constrained [6,27]. Regardless of particle specifics, the cold DM (CDM) implied hierarchical structure formation paradigm faces a number of challenges such as the angular momentum problem [52], the missing clusters [46] and satellites [41] problems, as well as the issue of missing stochastic gravitational wave background [65]. On the other hand, the modified gravity theories have to overcome well-posedness issues [70,75] and problems such as unstable stars [64] (see also Famaey & McGaugh [29] for other complications that specific theories have to contend with).

Since new physics are not readily forthcoming, it is perhaps worthwhile to revisit the question of whether the proven General Relativity (and its weak field limit), together with the known Standard Model particles, can possibly already account for some of the apparent DM (aDM) phenomenologies. This prospect may be viable due to the presence of autonomous gravitational fields not sourced by any matter, whose existence is in fact known since the early days [22,31] (see also e.g., Brill & Hartle [10] or Misner & Taub [51] for a curvature-singularity-free warped universe that's completely devoid of matter; for complex manifolds, we also have the well-studied Calabi-Yau manifolds [11,74]). However, when trying to explain the observation of mysterious gravitational content of the universe, that does not appear to interact through other forces, this most natural of possibilities somehow escaped close scrutiny (perhaps because the now dashed "WIMP miracle" and a desire for discovering new particles drew the discussion to new matter species from the beginning). Through our admittedly preliminary investigations in this paper, we hope to attract more attention to this less exotic explanation of the aDM phenomenology.

Turning to the specifics, we note that autonomous gravity must be carried within the Weyl curvature tensor[1] (since the Ricci curvature tensor equates to matter stress energy tensor), which contains not only gravitational waves (loosely, Newman-Penrose pseudo-scalars Ψ_0 and Ψ_4), but also a Coulomb piece (Ψ_2), usually in a difficult-to-disentangle jumble [76]. In other words, autonomous gravity configurations are not always simple nonlinear wave packets that can easily disintegrate. Geometrically, the Weyl tensor represents the variations in sectional curvatures[2] [33] (and Ricci their average), so its very presence is indicative of anisotropy and clumping, ideal for seeding structure formation, but it is simultaneously less prone (than CDM, which behaves more like pressure-less dust) to develop shocks or other sharp features [45] (otherwise vacuum black hole simulations using spectral methods would unlikely to have succeeded), as it is governed by the Bianchi identities.

When studying galaxies and clusters, Newtonian gravity is usually adopted. In this language, the autonomous gravity hides in the solutions to the homogeneous Poisson's equation. Specifically, although the metric perturbation component h_{tt} can be equated to an effective Newtonian-style potential $\Phi = -h_{tt}/2$ in the weak stationary field and slow motion limit, the Einstein's equations only reduce to Poisson's equation[3] $\nabla^2\Phi = 4\pi\rho_M$ and not all the way to Newton's law of universal gravitation. A solution to a linear inhomogeneous equation like Poisson's can be constructed out of two parts, a "particular solution" of the inhomogeneous equation, which $\Phi_N = -\int(\rho_M/\Delta r)dV$ produced by Newton's law qualifies as one, and a solution Φ_H to the homogeneous version of the Poisson's equation $\nabla^2\Phi_H = 0$ whose utility is to enforce boundary conditions (which need not be trivial in a cosmological context). Such a Φ_H field, although orphaned (not sourced by any matter), nevertheless generates a gravitational acceleration $-\nabla\Phi_H$, and when forcibly interpreted through Newton's law, would masquerade as a form of fake matter (henceforth referred to as the effective Weyl matter or EWM; since Φ_H is not sourced by local matter, it can only contribute to the Weyl half of the reconstructed – by using Φ as $-2h_{tt}$ – Riemann tensor), which must be dark as it cannot participate in Standard Model interactions.

For the weak field limit, once again recall that the higher order coupling between different sub-components of the overall potential Φ are negligible, so the governing equation for Φ is the linear Poisson's equation, for which solutions can be superimposed linearly, thus the EWM clouds are decoupled from matter-generated gravity and each other at leading order (but the matter can see the EWM at this order through the geodesic equations), allowing a dissociation of the gravitational and X-ray luminosity centers in the Bullet Cluster [16]. However, general relativity (GR) is ultimately nonlinear, so given sufficient interaction time, different EWM clouds and matter-generated gravity can eventually couple at higher orders, possibly contributing to the more complicated post-slow-speed-collision aDM distributions of the Train Wreck [38] (relative velocity at 1077km s^{-1} vs Bullet's 4700km s^{-1} [50]) and, to a lesser extend, Musket Ball [19] (1700km s^{-1}) clusters.

Further complications arise when one realizes that our universe may not have a full set of non-singular boundaries (e.g., its spatial slices may be large three dimensional spheres), in which case the boundary conditions for the metric or Φ become missing or effectively cyclic (which is also not very constraining). However, in full GR, the gravitational fields are endowed with geometric significances, so additional topological constraints arise to fill the gap (spacetime cannot just bend arbitrarily if it is to close up into the correct topology). Imagine an idealized compact boundary-less universe (similar considerations can be applied to individual spatial slices), whose Chern-Pontryagin density [4] ($R^a_{\ bcd}$ is the Riemann tensor, ϵ the Levi-Civita pseudotensor and $C^a_{\ bcd}$ the Weyl curvature tensor)

$$\rho_{CP} \equiv \frac{1}{2}\epsilon^{cdef}R^a_{\ bef}R^b_{\ acd} = \frac{1}{2}\epsilon^{cdef}C^a_{\ bef}C^b_{\ acd}\,, \tag{1}$$

---

[1]   Ordinary matter can also generate this type of curvature, so not all of it is autonomous, but all autonomous gravity is Weyl, because the Ricci tensor equates directly to the matter (incl. cosmological constant) stress-energy tensor.

[2]   The Gaussian curvature of the various 2-D geodetic surfaces developed out of 2-D planes in the tangent space of the spacetime at any location.

[3]   We work under a geometrized unit system where $G = 1 = c$, with kiloparsec being the fundamental length unit.

and Gauss-Bonnet invariant (R is the Ricci scalar)

$$\rho_{\text{GB}} = \sqrt{-g}\left(\frac{2}{3}R^2 + 2R_{ab}R^{ab} - C_{abcd}C^{abcd}\right),\qquad(2)$$

integrate into the instanton number [55] and $32\pi^2$ times the Euler characteristic [15] respectively, both of which are small integers for simple topologies. In other words, the average amplitudes of ρ_{CP} and ρ_{GB} should be on par with the inverse of the spacetime's volume. However, a cosmological constant Λ can create a surfeit of ρ_{GB} (via $R_{ab} = \Lambda g_{ab}$) if the size of the universe is greater than $1/\sqrt{\Lambda}$ (~ 10Gly for the real thing). In order to achieve a recalibration of ρ_{GB} without inadvertently bloating ρ_{CP}, two new gravitational components should be introduced, at commensurate abundances to each other and to Λ, so near-cancellations can occur. The EWM and ordinary Standard Model matter are the obvious choices.

Incidentally, this desirability for two separate new ingredients is not apparent when examining the specific Friedman-Lemaitre-Robertson-Walker metric, whose oversimplifying assumption of exact isotropy artificially take the Weyl half of GR and ρ_{CP} out of action (there is no way to arrange the principal null directions of the Weyl tensor [59] without breaking isotropy, or equivalently one can invoke the previous sectional curvature argument). In reality, the anisotropy on small scales are boosted by the two derivatives (multiplications by wavenumbers in momentum space) taking us from metric to curvature, so Weyl is far from negligible even with near-isotropy on large scales. In any case, regardless of whether this balancing act required by the compact example describes our actual universe, there is no reasoning that prevents the EWM from being present in it anyway.

2. Effective Weyl matter phenomenology

2.1. Overview

To execute a preliminary assessment of the admissibility of the EWM as an aDM candidate, we examine the galaxy rotation curves that helped launch the field of DM research in the first place. As the assumptions of weak stationary field and slow motion (as compared to the speed of light c) are reasonable, we can simply use the effective potential formalism (recall this is more general than Newton's law), and superimpose the potentials or accelerations from different origins.

Before going into any details, it is worthwhile re-emphasizing that we are not proposing a new modified theory of gravity. We are working completely within GR (and its weak-field slow-motion Newtonian limit). The governing equation that we solve is simply the Poisson equation $\nabla\Phi = 4\pi\rho_{\text{M}}$ (whose solution is $\Phi = \Phi_{\text{H}} + \Phi_{\text{N}}$, with Φ_{H} being the solution to the homogeneous version of the equation, and Φ_{N} the particular solution to the inhomogeneous equation) satisfied by the Newtonian gravitational potential, which has dominated gravitational physics for centuries. What we are doing differently is that we also consider those solutions to this equation that have previously been thrown away due to oversimplified boundary conditions (i.e., we are not changing any theories, just trying to make sure that the relevant solutions are not inadvertently discarded).

The potential issue with boundary conditions we explore is that traditionally in astrophysics, it had been second nature to assume that the object in focus can be studied in isolation. For example, when trying to solve the gravitational field inside a star, we often assume that it is sitting all by itself in an otherwise empty universe, so that the gravitational field comes only from the star itself and drops to zero when we are far away from the stellar surface (such an asymptotically vanishing boundary condition end up setting $\Phi_{\text{H}} = 0$). This is not always valid of course, since the surroundings of the star may not really be negligible (e.g., the star may be in a binary with a black hole), and may exert strong influences on the interior of the star (e.g., tidally deform it). Inside the star then, such external influences manifest through a non-vanishing Φ_{H}, since they are not sourced by matter inside of that star. Similarly with galaxies, their rotation curves had traditionally been examined by

assuming that the galaxies exist in isolation (i.e., the gravitational field is implicitly assumed to vanish at large distances, thus setting $\Phi_H = 0$), even though we now know that they must be subsumed into larger-scale gravitational structures like clusters and filaments, so we must have $\Phi_H \neq 0$. In fact, the aDM seen in these larger structures could also be of Φ_H in nature (i.e., not sourced by the matter content within the clusters etc), which are themselves determined by the boundary and initial (since at the largest scales, we cannot assume stationarity) conditions of the universe (please refer to the discussions in Sec. 1). When zooming in on an individual galaxy then, these cluster Φ_H serve to produce non-trivial boundary conditions on the region around that galaxy, which we carve out as the computational domain to solve the Poisson equation in.

Our new ingredient helping to explain the rising tails of the rotation curves is simply this non-vanishing Φ_H, which has always been allowed by the Newtonian limit of GR (although Newton's law is narrower in scope than the Poisson's equation and only gives Φ_N), but had unfortunately been thrown away by the implicit assumption that galaxies exist in isolation. When elevated back to GR language, this Φ_H must be a part of the Weyl curvature tensor, because it is not sourced by in-situ matter (the other half of the Riemann tensor, namely the Ricci tensor, must equate to the matter stress-energy tensor and thus cannot correspond to Φ_H). Therefore, in the bigger picture, the Φ_H we consider below in the more specialized context of individual galaxies (explaining galactic scale aDM phenomenology) is also an integral part of the autonomous gravitational content of the universe (explaining aDM phenomenology on all scales).

With autonomy, Φ_H brings with it genuine additional freedom, which means that the present framework is more flexible than modified gravity theories such as modified Newtonian dynamics (MOND), which keeps $\Phi_H = 0$ and instead adjust the dependence of Φ_N on matter, and therefore doesn't really add any freedom unless this dependence is allowed to vary from situation to situation. As we have discussed in Sec. 1, this freedom allowed a decoupling between Φ_H and Φ_N, and thus consistency with the Bullet cluster observations. Another place where such flexibility may prove useful is when aDM exhibit variations across galaxies. E.g., if the claim of a DM-less galaxy by van Dokkum et al. [26] turns out to be valid, then the present framework can easily accommodate it if the local environment within the galaxy cluster is such that the galaxy in question experiences boundary conditions that lead to a vanishing Φ_H (i.e. the galaxy is more isolated from its siblings than usual). We caution though, an alternative explanation is that since the EWM only becomes important at large galactocentric radii (see below), and observations of distant galaxies may simply be seeing only the brighter central core, so the lack of aDM may just be that the EWM dominated regions are not seen.

2.2. A galactic effective Weyl matter solution

Our autonomous gravity component mimicking a galactic aDM halo is the very simple axisymmetric solution **(this form provides a rising tail without introducing any singularities or discontinuities in the potential, in particular, the lack of a singularity at the origin fixes the powers)**

$$\Phi_H = \frac{\kappa}{2}\rho^2 - \kappa z^2 \tag{3}$$

to the homogeneous Poisson's equation, which in the cylindrical coordinates $\{\rho, \phi, z\}$ reads

$$0 = \nabla^2 \Phi_H = \frac{1}{\rho}\frac{\partial}{\partial \rho}\left(\rho \frac{\partial \Phi_H}{\partial \rho}\right) + \frac{1}{\rho^2}\frac{\partial^2 \Phi_H}{\partial \phi^2} + \frac{\partial^2 \Phi_H}{\partial z^2}. \tag{4}$$

The gravitational acceleration associated with this solution is given by

$$g_\rho = -\kappa\rho, \quad g_\phi = 0, \quad g_z = 2\kappa z, \tag{5}$$

and it is simple to double-check that the flux of this acceleration across the surface of any pillbox surrounding the galaxy (the galactic plane is assumed to be at $z = 0$) vanishes, so there is no mass sourcing it. This gravitational field is supported instead by the boundary conditions where the galactic aDM halo subsumes into the aDM distribution for the entire cluster (note studies revealing a collusion between the halos of different galaxies in the lensing data [47], in their orientations [68], and on missing aDM in the local universe [39] suggest that these individual halos should not exist in isolation, but instead form an interconnected whole).

It is interesting to note that such boundary conditions (can be recovered by taking ρ and z to large values in Eq. (3)) would entail larger acceleration values in the galactic corona, providing a possible mechanism to produce the highly energetic ($10^5 - 10^6$K) gases found in those remote regions. Concentrating on the galactic plane where we have more tracers and data, we note that the component g_ρ (g_z will be discussed in Sec. 2.4) along the plane increases linearly with ρ, translating into an "extended DM core" in the CDM terminology (i.e., a constant ρ_{aDM} spherical density profile; there is thus no cuspy halo problem [20] in the galactic center), which has occasionally been noted in literature (see e.g., [17,40]) to be able to provide better fits to data than CDM-based profiles (e.g., Navarro et al. [53,54]). To see the direct effects of g_ρ, we need to go to very large ρ and study the tails of the galaxy rotation curves, which we turn to examine now.

2.3. Anatomy of rotation curves

Rising tails at large galactocentric radii ρ are seen for a large number of rotation curves (see the many references in Ruiz-Granados et al. [62]), yet such a trait can not be explained with the theoretically modelled CDM profiles nor MOND [49], which predict curves that are flat or declining at very large ρ [14,40]. This is a cause for concern given that the tail is particularly informative, because while uncertainties in ordinary matter distribution (e.g., those associated with stellar mass-to-light ratios and the molecular gas densities) complicate interpretation of the inner and intermediate segments of the rotation curves, their impacts usually do not extend to the far outer regions, which consequently reflect the properties of the aDM in a more transparent manner.

We caution though that whether a rising tail is universal across all galaxies has not been firmly established. Exploratory examinations of the extreme outer edges of the galaxies are not receiving sufficient observation time allocations, so it is possible that the absence of a rising tail from some curves may simply be due to data points not extending far enough out **(by definition, the rising tails are regions where baryonic matter becomes subdominant, so there are few baryonic tracer objects to measure the rotation speeds with; further in from the tails, a $\sim 1/\sqrt{r}$ dropoff from baryonic contribution combines naturally with a $\sim r$ rising aDM contribution into a rather flat curve in the transition zone where the two are of comparable strengths)**. We note in addition that our study can be used to infer an estimate on when would the rising tails appear (since κ appears common across galaxies, see below for details), and so is easy to verify or falsify with large scale observation campaigns of the galaxy outer regions. More confusingly, with the existing surveys, people had been more interested in declines in the curves associated with mass distribution cut-offs, so rising tails are instead interpreted as "asymptotically approaching a flat curve after a temporary dip" **(see many examples of this morphology in the agnostic sample of curves in Wojnar et al. [71]; such a downwardly convex shape is natural when the declining baryonic dominance transitions into the rising EWM dominance regime)** and used to exclude declines, while continuously rising curves are interpreted as "haven't yet reached the flat part by the last measured point" (see e.g., the first paragraph of Sec. 7.1 in de Blok et al. [21], and also their Fig. 57 which in fact display many curves with rising tails). In other words, general statements that curves are consistent with being asymptotically flat does not in fact exclude rising tails, and a careful inspection of the morphological details of actual individual curves is still required. This reality reflects the extreme incompatibility of rising tails with CDM or modified gravity, that many authors didn't even consider them a possibility, and instead unconsciously interpreted them out of existence.
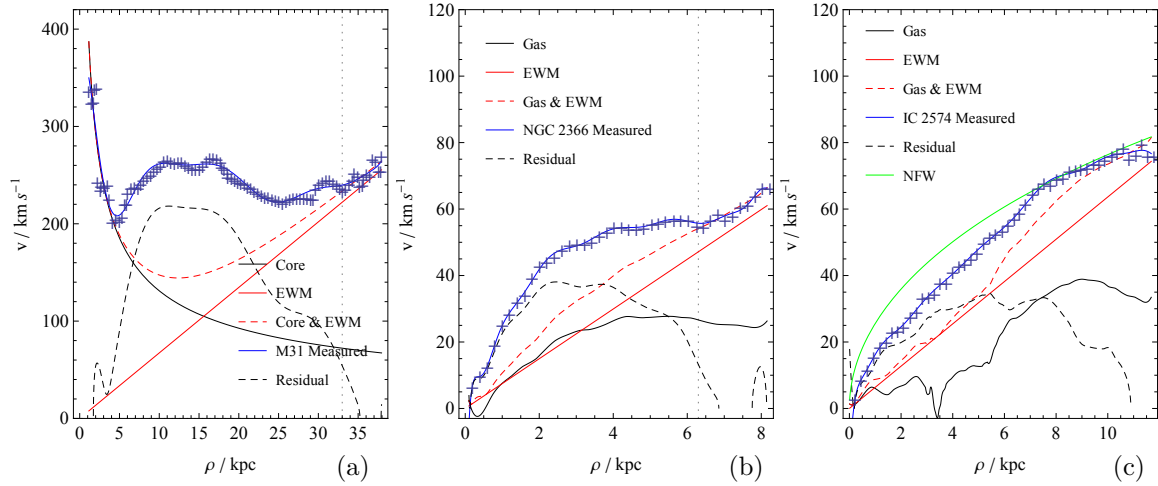
Figure 1. The fitted rotation curves for (a): M31 with $\kappa = 5.035 \times 10^{-10}\text{kpc}^{-2}$, and $M = 4 \times 10^{10}\text{M}_\odot$, (b): the dwarf galaxy NGC 2366 with $\kappa = 6.215 \times 10^{-10}\text{kpc}^{-2}$, and (c): the dwarf galaxy IC 2574 with $\kappa = 4.5 \times 10^{-10}\text{kpc}^{-2}$. The blue crosses are the HI-implied rotation speeds taken from Chemin et al. [14] and Oh et al. [56], and the blue curves their polynomial interpolations. The black curves in panels (b) and (c) are the measured gas contributions from Oh et al. [56]. The green curve in panel (c) is a CDM profile fit (see Fig. 6) demonstrating that such profiles tend to overshoot the observed rotation curve. Note the rotation speeds add in quadrature, so accelerations add linearly.

A rising tail is however natural with an EWM-generated linearly rising $|g_\rho|$. For concreteness, we carry out fits for a few example galaxies where high quality data for the rotation curve are available. Before starting though, we caution that there is significant difficulty with fitting to rotation curves, since besides the aDM contributions, there are also other unknowns like mass-to-light ratio or molecular gas. Even if measurements of "all" relevant quantities are available (which as far as we know is not the case for any galaxy, since for the very least the molecular gases are difficult to see), they would contain large uncertainties, so it is not quite optimal to produce least square fitting wellness parameters for entire curves, since the goodness of fits will have to be interpreted conditional on the aforementioned uncertainties associated with all the baryonic parameters. So the statistical significances of the fits are substantially degraded, rendering the fits much less informative. However, it is possible to make more robust quantitative measurements based on particular segments of the rotation curves. In particular, because baryonic matter density drops with increasing galactocentric radius ρ, their contribution to the overall rotation curve must rapidly decline, so for the tail section of the curves that we are interested in, uncertainties related to baryonic matter fortunately becomes subdominant. Therefore, by concentrating on the tail section, it becomes possible to make robust assessments, for which the impact of baryonic matter uncertainty is minimized (if for specific galaxies, high quality data on certain baryonic components are available, it also doesn't hurt to explicitly take them into account, so as to further reduce the uncertainty, a strategy that we will adopt with our examples below). Specifically, to quantitatively gauge how well the EWM profile performs, we note that Eq. (5) predicts a linearly rising EWM contribution to the rotation curve, that in addition, must pass through the origin (i.e. $v = 0$ when $\rho = 0$). In other words, while even the simplest linear fit to the tail will produce two parameters, the slope and the intercept, the EWM profile is so rigid that it only has one parameter κ that can be adjusted. This "over-determinancy" translates into a rather stringent test for the EWM profile - if not correct, there is no way it will match both the slope and the intercept of the linear fit with a single parameter. We can also produce a quantitative measurement of this statement, namely by how much does the slope of the EWM fit (varying only κ) differs from the slope of the best linear fit (varying both slope and intercept).

We begin with the nearby (thus good data quality) M31 (Andromeda). Our fitting procedure is as follows

1. Because M31 exhibits a strong bulge influence, it becomes possible to infer a bulge mass by fitting to the very inner part ($\rho < 5$kpc) of the rotation curve. This is done because as discussed in the last paragraph, any reduction in the uncertainty about baryonic contributions will further reduce the errors when we fit to the tail section. The bulge contribution is modelled as a mass monopole $\Phi_{\mathrm{Nb}} = -M/\rho$, and by inspection we obtain $M \approx 4 \times 10^{10} \mathrm{M}_\odot$. See Fig. 1(a) for the fitting results.

2. We then turn to the tail section (beyond the dotted vertical line in Fig. 1(a) at around 33kpc). We begin by taking off the monopolar bulge contribution, so that the remainder contains the contribution from the EWM (dominate) and the other non-bulge baryonic components (subdominant).

3. A fit for κ is then carried out. Eq. (5) predicts a EWM contribution to the tail of the rotation curve at $v = c\sqrt{\kappa}\rho$ (where the speed of light c is in units of km/s), and we fit this functional form to the monopole-removed tail section of the rotation curve. The fitting is done using the standard computation package `Mathematica`, yielding best fit $\kappa = 5.035 \times 10^{-10} \mathrm{kpc}^{-2}$. For comparison with a full linear fit, it is more convenient to present the result in terms of the overall slope $c\sqrt{\kappa}$, whose best fit value is 6.732, with standard error 0.0498.

4. The highly rigid nature of the EWM profile (containing only one free parameter) as compared to CDM profiles (containing many tunable parameters) allows us to carry out a test on whether its rigid functional form matches data. Namely, as discussed previously, we can carry out a full linear fit to the tail with $v = a\rho + b$ and see whether a is close to the fit for $c\sqrt{\kappa}$ we obtained during the last step, and whether b is close to zero. Recall though the tail still contains non-bulge baryonic contributions, and they would contribute to b; nevertheless since they are subdominant in the tail section, b shouldn't be large. Our fitting yields the best fit slope at $a = 5.96$, with standard error 1.29, which matches rather well with the $c\sqrt{\kappa}$ obtained earlier (well within one standard error). The parameter b has a best fit value of 27.65 and a standard error of 46.36, which is also consistent with a nearly vanishing intercept.

5. Finally, a few words regarding the mid-section of the rotation curve is in order. The remaining miscellaneous contributions, from those stars, dust and gas residing outside of the central core, are collected into the "residual" in Fig. 1(a). We caution that the study by Bournaud et al. [9] on recycled dwarf galaxies suggests the presence of large amounts of difficult-to-see cold molecular gas in the discs of their parent spiral galaxies (see also e.g., Li et al. [44] for more direct observational evidences), thus there is likely still an invisible matter component in the aDM (but of a mundane variety; being ordinary matters, their amounts and distributions could also differ substantially between galaxies of different types and ages, just as stellar matter would) that contributes to the inner to intermediate regions of the rotation curves.

   Note further that all these aforementioned components are spread out on a disc, and not distributed in a spherically symmetric manner, so the residual curve is not bounded from below by a Keplerian profile. Instead, a rapid $\sim 1/\Delta\rho$ decline near a high matter density strip, $\Delta\rho$ being the distance to the sharp edge of the strip, provides a better approximation (and a slower decline in the orbiting speed is to be expected if the drop-off in density is more gradual), and is consistent with Fig. 1(a).

Beyond bulgy disc galaxies like M31, it is also interesting to examine dwarf galaxies. Because they are aDM-dominated, their entire curves should behave much like the tail, continuously rising throughout the available data range, a trend that is indeed seen in e.g., Fig. 57 of de Blok et al. [21]. Here, we examine in more details two galaxies investigated by Oh et al. [56], which had been careful to scrub the contaminations due to non-circular motion (a significant problem with dwarfs) from their rotation curves. Beginning with NGC 2366 (Fig. 1 (b)), we note that it exhibits a pronounced tail section, which is once again well accounted for by the EWM profile. In contrast, even empirical CDM profiles proposed to resolve the cuspy halo problem can not fit to it (see Fig. 22 in Oh et al. [56]). Our detailed fitting procedure follows closely that of M31 and are as follows

1. The rotation curve does not contain a clear bulge-dominated inner segment, so we cannot infer a bulge monopole size, but this also means the bulge should not be significant (recall that we are dealing with a dwarf galaxy). Instead, carefully analysed gas contribution derived from the integrated H I map is available for this galaxy, so we explicitly account for this contribution.

2. Turning to the tail section, we once again remove the contribution from the known baryonic component, gas this time, so as to maximally scrub down the tail to a cleaner EWM domination. We then fit for κ with the same procedure as was done with M31, yielding best fit κ at $6.215 \times 10^{-10}\mathrm{kpc}^{-2}$. Note that despite the drastically different nature of the galaxies (massive spiral versus dwarf) and different rotation speeds (hundreds of km/s versus dozens), the κ values are remarkably similar between NGC 2366 and M31, differing by only 25% rather than orders of magnitude.

3. The κ value translates into a slope $c\sqrt{\kappa}$ at 7.47916, with standard error 0.0518. The full linear fit on the other hand yields a slope of $a = 6.907$ with standard error 0.600, as well as an intercept $b = 4.169$ with standard error 4.356. Once again, the EWM's rigid form is consistent with the morphology of the tail section of the rotation curve (a and $c\sqrt{\kappa}$ agree within one standard error and b is consistent with being nearly zero).

4. The uncertain stellar contributions for this faint dwarf galaxy are collected into the residual.

For the fainter IC 2574 (Fig. 1 (c)), we need a somewhat different fitting procedure:

1. Once again, the gas contribution from the integrated H I map is available. However, this time the gas contribution rises very rapidly on the outer regions, so we end up with a large and varying gas contribution in the tail. This unfortunately obscures the linear EWM tail there (the curve bends downwards following the trend in the gas contribution). Nevertheless, the gas contribution declines at the extreme large ρ end, while EWM keeps rising to greater dominance there, so we can adopt a simpler procedure by letting the EWM match the last point in the rotation curve. This yields $\kappa = 4.5 \times 10^{-10}\mathrm{kpc}^{-2}$, differing from the value for M31 by only around 10%, despite the very different galaxy types and rotation curve morphology.

2. The very different (as compared to Fig. 1(a) for massive spiral galaxies), continuously rising rotation curve morphology (also more or less shared by NGC 2366) seen for the dwarfs is because for these aDM dominated dwarf galaxies, the EWM contribution is significant throughout the entire curve, even on the inside. The almost linearly rising curves thus provides a rather direct support for the rigid linear EWM profile. In contrast, they pose a serious challenge to common theoretical CDM profiles that flatten off at large ρ, as they cannot provide sufficient speed on the outside without overshooting the inside. Since it is difficult to produce outward acceleration, overshooting is a more troublesome problem. In Fig. 1(c), we provide a demonstration of this difficulty by making a Navarro-Frenk-White [53] profile fit as a green curve. The fitting is done by inspection for the tail of the curve beyond $\rho \sim 7\mathrm{kpc}$, yielding parameter values $v_{200} = 160\mathrm{km/s}$, $\mathcal{C} = 1$, and $R_{200} = 100\mathrm{kpc}$, feeding into

$$v_{\mathrm{NFW}}(\rho) = v_{200}\sqrt{\frac{\ln(1+\mathcal{C}x) - \mathcal{C}x/(1+\mathcal{C}x)}{x\left(\ln(1+\mathcal{C}) - \mathcal{C}/(1+\mathcal{C})\right)}}, \tag{6}$$

where $x \equiv \rho/R_{200}$. Note that even though we have tried to suppress the overshooting by reducing $\mathcal{C}$ to a perhaps unrealistically small value (it is around $10 - 15$ for the Milky Way) and by making R_{200} very large (beyond this value, the CDM profile turns downwards), the inner regions of the CDM predicted curve still rests significantly above the observed rotation curve.

As already alluded to, the κ values for all three galaxies are quite similar, which could be understood in the EWM context as due to κ being determined by the fairly common general conditions in a local neighbourhood of the cluster that set the boundary conditions for the individual galactic halos (both dwarf galaxies reside in the nearby M81 group and M31 is in our local group; furthermore, the

supra-galactic structures within the local group – e.g., planes of dwarf galaxies – have been shown to possess curious alignments [58], so the individual galaxies must all subsume into a common larger cluster scale structure). We obviously can not claim a quasi-universality of κ based on data from only three galaxies (the scrubbing technique of Oh et al. [56] should be applied to more galaxies to boost the statistics), but nevertheless note that it would be quite a coincidence if the commonality shared by these three rather arbitrarily chosen cases is purely accidental, given that the galaxies belong to different classes as well as exhibit different rotation curve morphologies and average speeds. Even more fortunately, establishing the universality of κ does not require us to obtain the full rotation curves. At very large galactocentric radii, EWM would dominate, leading to a linear $v = \sqrt{\kappa}\rho$ and thus a constant angular velocity $\sqrt{\kappa}$ (using our average $\kappa \approx 5.3 \times 10^{-10}\text{kpc}^{-2}$ from the three galaxies examined above, this translates into a rotation period for the outer rims of galaxies at about 0.89Gyr). Therefore, with H I and other measurements of the outer regions of the galaxies, one should record a universal rotation period, shared between all galaxies regardless of their masses and the radii at which we happen to observationally take readings (such universality would not be present with truly asymptotically flat rotation curves), which matches and provides a robust (without needing additional assumptions such as sharp truncations of the discs) explanation for the observational results reported in Meurer et al. [48] for large sample sizes. Alternatively, recall that the EWM profile resembles that of a spherical CDM halo with a constant density proportional to $\sqrt{\kappa}$ (i.e., an extended core), the universality of κ across different galaxies then implies that the characteristic volume density (the overall scaling factor) in best CDM fits should be roughly constant, which is indeed observed to be the case for samples spanning over five decades of galaxy luminosity [43].

Furthermore, this universality in κ also provides a simple explanation for the well-known relationship between specific angular momentum $j = J/M$ of a galaxy and its total stellar mass M, namely that $j \propto M^{0.6}$ [28]. In the present consideration, we have that, for measurements where baryonic influence does not overwhelm the EWM contribution to the rotation curve (failure of this simplifying condition feeds into the rather significant scattering in the observed j vs M relation), we can approximate the galaxy as a rigidly rotating disk with angular velocity $\sqrt{\kappa}$ and some distribution of stellar mass density, say exponential $\rho_* = \rho_{\text{core}} \exp(\rho/H)$, where H is some scale distance. Then simple integration gives

$$j = \frac{6}{6.28} \frac{M\sqrt{\kappa}}{\rho_{\text{core}}}, \tag{7}$$

where the central stellar mass density ρ_{core} is unsurprisingly dependent on M as well, with $\rho_{\text{core}} \propto M^{0.42-0.74}$ observed for early type galaxies [63]. Therefore, despite extreme crudeness, our estimate can already produce a $M^{0.6}$ power law, while it should be clear as well that, if the angular velocities of galaxies are completely arbitrary, we would not be able to obtain a clean dependence on M alone. Note also that the functional form of Eq. (7) is not sensitive to the detailed morphology of the galaxy due to dimensionality, but the precise numerical coefficient is, which implies that disk and bulge dominated galaxies should naturally lie on two different parallel lines in a $\log j$ vs $\log M$ plot, as is indeed observed.

Another simple estimate shows that the universality of κ also leads to the baryonic Tully-Fisher relation [?]. Note first that the flat part of the rotation curve corresponds to where the decline and increase in v arising from the baryonic and EWM contributions balance out, leading to (at sufficiently large ρ, the bulge and disk contribution to v can be approximated by a $1/\sqrt{\rho}$ profile)

$$\frac{dv}{d\rho} = \frac{d}{d\rho} \sqrt{\frac{GM_{\text{bar}}}{\rho} + c^2\kappa\rho^2}\bigg|_{\rho=\rho_{\text{f}}} = 0, \tag{8}$$

where ρ_{f} signifies the flat part of the rotation curve. Solving for ρ_{f}, and substituting into the rotation speed for that flat region, we have then

$$
\begin{aligned}
v_{\mathrm{f}} &\equiv \left. \sqrt{\frac{GM_{\mathrm{bar}}}{\rho} + c^2 \kappa \rho^2} \right|_{\rho=\rho_{\mathrm{f}}} \\
&= \frac{\sqrt{3}c^{1/3}}{2^{1/3}} \kappa^{1/6} \left(GM_{\mathrm{bar}}\right)^{1/3},
\end{aligned}
\tag{9}
$$

or in other words $M_{\mathrm{bar}} \propto v_{\mathrm{f}}^3$ when κ is common across galaxies. This power is consistent with the measured value of 2.99 ± 0.2 given by ?], which accounted for mass-to-light ratio effects (without this step, the power comes out at around 3.7).

2.4. Off the galactic plane

A very distinguishing feature of the EWM as described (to lowest order approximation) by Eq. (5) is the fact that the EWM is "repulsive" off the galactic plane. More specifically, g_z is pointed away from the galactic plane, with an increasing strength at larger $|z|$, so it tends to (very slowly, typical value for EWM acceleration is $\kappa \times 1\mathrm{kpc} \sim 10^{-12}\mathrm{ms}^{-2}$ in SI units) remove matter that are not close to this plane or become dislocated from it (e.g., during galactic mergers), thus may possibly help to chisel out and maintain superthin pure-disc galaxies through the many mergers that they likely would have experienced (in order to grow to their present sizes), which the CDM framework struggles to account for [42,52].

Note though, the gravitational pull from regular disc matter points in the opposite direction to g_z, so the stable disc plane is thickened. As some of that disc matter is dim and possibly lumped into aDM contribution, one may even on occasions infer that there is an overall dark attractive force towards the disc. The relative weakness of the "repulsive" g_z is even more pronounced in the core region, where the high concentration of ordinary matter dominates (see Fig. 2 below). EWM thus contributes little to bulge dynamics, and certainly would not send the bulge matter flying away (large elliptical galaxies share similar dynamical characteristics to the bulges of disc galaxies, and their older age likely implies greater proportions of dim ordinary matter – as molecular gases as well as compact objects – whose distribution and density are unfortunately uncertain). In short, absent major events such as mergers knocking (mostly gaseous) matter into high $|z|$ regions, one should not expect to see significant outflows away from the galaxy when it is resting in a quiescent state.

Even during extreme events such as mergers, the dislocated material does not simply launch vertically into deep space. The combined acceleration directions from the EWM and the massive core of ordinary matter is plotted in Fig. 2. We see that there are two regimes[4]: (1) matter starting off closer to the disc gets pushed towards the galactic center, but does so by first being carried to higher latitudes and then compressed nearly radially towards the galactic core; (2) matter starting off/knocked out sufficiently far from the disc would eventually get launched into deep space (which possibly explains how metals arrive at large distances of over $150\mathrm{kpc}$ from the galactic centers [69]), but in a direction more closely hugging the rotation axis of the galaxy.

Spiral galaxies such as the Milky Way would frequently experience minor mergers with dwarf galaxies, during which stars (and gas) from the spiral galaxy would inevitably become dislocated off the disk and into region (1), and subsequently become lifted to moderately high galactic latitudes by the EWM field. The region (1) halo stars thus produced should, and have in fact been observed to, retain some features indicative of their disk ancestry, e.g., in their chemical composition [7], and prograde rotation [12]. Much of the stellar debris originating in the tidally-disrupted dwarf galaxy will

---

[4]   Note for simplicity we had not included the matter contribution from the extended disc. Including it will not change the basic picture apart from pushing the separatrix streamline further up, enhancing the size of regime (1). The plot also does not include the centrifugal forces arising from any circular motion, which would be particle specific.
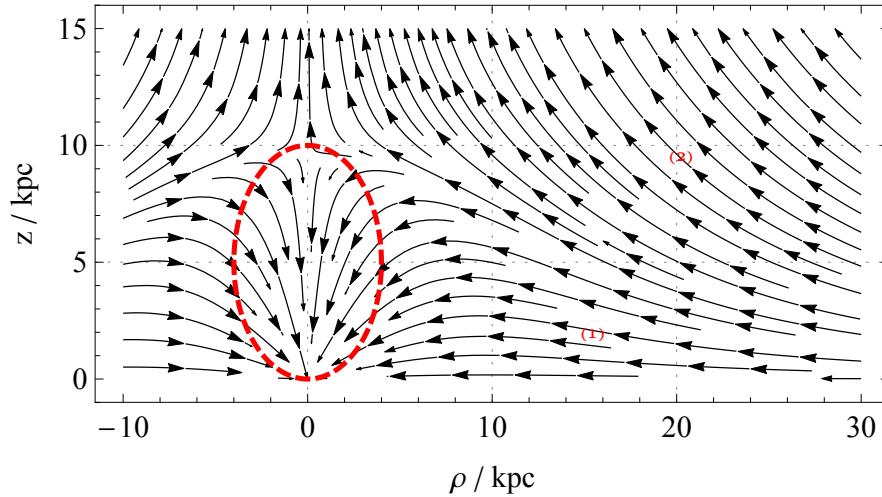
Figure 2. The streamlines of the combined acceleration acting on off-galactic-plane particles, due to the galactic core mass M and the EWM parametrized by κ. The values of these parameters are taken to approximate the Milky Way, with $\kappa = 5.3 \times 10^{-10} \text{kpc}^{-2}$ being the average of the three galaxies from last section (in the same cluster as the Milky Way), and $M = 2 \times 10^{10} \text{M}_\odot$, since the overall mass of the Milky Way is about half of that of M31. The red dashed circle signifies the boundary of the Fermi bubble. The coincidence between the bubble and separatrix heights may be accidental, or alternatively the hardness of the X-ray emissions (Loop I, residing further out, has a softer spectrum) may depend on whether the EWM driven ambient and AGN/starburst driven burst flows are counter-streaming (relevant for shock wave properties).

however fall into region (2) and form a distinct outer population of halo stars with lower metallicity. The existence of this dichotomy of halo star populations is supported by observations (see e.g., Carollo et al. [12], Hartwick [34] and references therein), and the boundary between their spatial distributions is indeed located at around $10 - 15$kpc from the galactic center, matching that dividing EWM regions (1) and (2) shown in Fig. 2 (i.e., the two EWM regions correspond to the observed inner and outer halos, respectively).

In the radial direction, the stars and gas knocked into region (1) are guided towards the galactic center, helping to feed the growth of the supermassive black hole, leading to the consequence of an under-abundance of luminous matter in the disc as compared to the sizes of the supermassive black holes, which would then appear more massive than expected from a traditional CDM-based co-evolution scenario (see e.g., Wu et al. [72]). Because merger events are episodic, the galactic core is fed material in discrete bursts. This could provide clues to the missing pieces in the formation mechanism of the mysterious Fermi bubbles [25,67]. These are giant structures seen above and below the galactic center (schematically marked out by the red dashed line in Fig. 2) in γ-rays, microwave and polarized radio signals [13,30,60], as well as in X-rays [66]. Digging through the archaeological evidences found within the bubbles, it has been suggested that they are outflows driven by a single past episode of active galactic nucleus (AGN) outburst and/or starburst activity occurring in the galactic core a few million years ago [1,8,67]. However, there is currently no contemplation as to where the extra material falling into Sgr A^* and/or driving the star formation activities came from in the first place, and why it is supplied in a short discrete burst. We note though, that there are evidences for several recent minor mergers where the Milky Way had absorbed smaller galaxies, and when driven by the EWM, dislocated gases will take at least (centrifugal forces will likely prolong the journey) a quarter of a billion years to arrive at the galactic core, largely regardless of where they started off (solution to $d^2\rho/dt^2 = -\kappa\rho$ is $\rho = \rho_0 \cos(\sqrt{\kappa}t)$, so $\rho = 0$ when $t = \pi/(2\sqrt{\kappa})$, independent of initial ρ_0). Therefore, an initially diffuse plume will automatically compactify into a small extent in ρ and feed either or both of the aforementioned AGN and starburst activities in a bursty fashion. Furthermore, this timetable is broadly

in line with e.g., the previous crossing of the Milky Way's galactic disc by the Sagittarius dwarf galaxy (est. 0.85Gyr ago, see Purcell et al. [61]).

In addition, gravitational lensing may also provide clues to the structure of the aDM off of the galactic plane, if the lens galaxy is viewed edge-on. Fig. 2 shows that the EWM should produce a quadrupolar contribution to the overall lensing potential (the acceleration field is the gradient to the potential; also recall that Fig. 2 includes a monopolar contribution from the galactic core, which should be removed for the present consideration), essentially acting as an enhancement to the disc contribution (a monopole plus a quadrupole at the lowest orders), which may be powerful enough to resolve the radio flux-ratio anomalies. Specifically, the brightnesses of the multiple images of a lensed object often do not match traditional ellipsoidal CDM predictions based on the locations of the images (see e.g., Goobar et al. [32] for an arbitrary example). This discrepancy is difficult to explain even when additional dark substructures are introduced into the modelling of the lens galaxies [73], as the CDM predicted substructure abundance is insufficient to account for the high incidence rate of such anomalies. It has been noted though by Hsueh et al. [35,36,37], that an edge-on disc can possibly help make up for the residual, provided the discs are massive enough (such masses are currently observationally unavailable). The present consideration offers another alternative, namely that the smooth galactic EWM, behaving much like a very massive disc in terms of producing higher multipoles in the lens potential, accounts for most of the anomalies (other factors such as free-free absorption makes up the remainder), leaving little need for injecting additional low mass dark substructures.

3. Conclusion

Galaxy rotation curves exhibit features that require gravitational contributions beyond those arising from Newton's law of universal gravitation. Through concentrating on places most directly reflective of said new ingredients, we demonstrate in this paper that they can possibly be introduced within our verified understanding of gravity and particle physics, by noting that the gravitational *field*, like in any other field theories, does not always require source terms to exist; it can also be sustained by non-trivial boundary and/or initial conditions. On even larger length scales, the loss of symmetries poses a technical challenge to the analytical analysis of the EWM, but constructs such as the integral curves of the Weyl tensor's characteristic directions [57] may provide useful tools for extracting general attributes, e.g., along the lines of [77]. On a broader note, as any numerical relativist working on binary black hole mergers would testify, gravity is not always a surrendering slave to matter (black holes can be excised from the computational domain since no information comes out, and the violently twitching exterior vacuum is what's being simulated), and if some of the aDM turns out to indeed be the EWM, the reverse may in fact be more true of our universe. Substantial efforts likely need to be invested to ascertain whether this is indeed the case, with the first steps perhaps being the establishment of whether a rising tail is indeed a universal feature among all galaxies, by carefully examining their large galactocentric radius regions with the next generation of more powerful radio telescopes. The present paper aims to solicit interest from experts of diverse backgrounds to investigate the crevices where GR may be hiding further surprises for us, resulting in the more nuanced features of this more mundane gravity theory having to be considered in place or in addition to other dark matter considerations.

References

1.   Ackermann, M., Albert, A., Atwood, W. B., et al. 2014, Astrophys. J., 793, 64

2.   Ackermann, M. et al. 2017, Astrophys. J., 840, 43
3.   Akerib, D. S., Alsum, S., Araújo, H. M., et al. 2017, Physical Review Letters, 118, 021303
4.   Alexander, S. & Yunes, N. 2009, Phys. Rept., 480, 1
5.   Aprile, E., Aalbers, J., Agostini, F., et al. 2017, Physical Review Letters, 119, 181301
6.   Asztalos, S. J., Carosi, G., Hagmann, C., et al. 2010, Physical Review Letters, 104, 041301
7.   Bergemann, M., Sesar, B., Cohen, J. G., et al. 2018, Nature, 555, 334
8.   Bordoloi, R., Fox, A. J., Lockman, F. J., et al. 2017, Astrophys. J., 834, 191
9.   Bournaud, F., Duc, P.-A., Brinks, E., et al. 2007, Science, 316, 1166
10. Brill, D. R. & Hartle, J. B. 1964, Physical Review, 135, 271
11. Calabi, E. 1954, Proc. Internat. Congress Math. Amsterdam, 2, pp. 206–207
12. Carollo, D., Beers, T. C., Lee, Y. S., et al. 2007, Nature, 450, 1020
13. Carretti, E., Crocker, R. M., Staveley-Smith, L., et al. 2013, Nature, 493, 66
14. Chemin, L., Carignan, C., & Foster, T. 2009, Astrophys. J., 705, 1395
15. Cherubini, C., Bini, D., Capozziello, S., & Ruffini, R. 2002, Int. J. Mod. Phys., D11, 827
16. Clowe, D., Bradač, M., Gonzalez, A. H., et al. 2006, Astrophys. J.l, 648, L109
17. Corbelli, E., Lorenzoni, S., Walterbos, R., Braun, R., & Thilker, D. 2010, Astron. Astrophys., 511, A89
18. Cui, X., Abdukerim, A., Chen, W., et al. 2017, ArXiv e-prints [eprint[arXiv]1708.06917]
19. Dawson, W. A., Wittman, D., Jee, M. J., et al. 2012, Astrophys. J. Lett., 747, L42
20. de Blok, W. J. G. 2010, Advances in Astronomy, 2010, 789293
21. de Blok, W. J. G., Walter, F., Brinks, E., et al. 2008, Astron. J., 136, 2648
22. de Sitter, W. 1916, Mon. Not. R. Astron. Soc., 77, 155
23. Dicus, D. A., Kolb, E. W., Teplitz, V. L., & Wagoner, R. V. 1978, Phys. Rev. D, 18, 1829
24. Dicus, D. A., Kolb, E. W., Teplitz, V. L., & Wagoner, R. V. 1980, Phys. Rev. D, 22, 839
25. Dobler, G., Finkbeiner, D. P., Cholis, I., Slatyer, T., & Weiner, N. 2010, Astrophys. J., 717, 825
26. van Dokkum, P. et al. 2018, Nature, 555, 629
27. Du, N. et al. 2018, Phys. Rev. Lett., 120, 151301
28. Fall, S. M. & Romanowsky, A. J. 2013, Astrophys. J. Lett., 769, L26
29. Famaey, B. & McGaugh, S. 2012, Living Rev. Rel., 15, 10
30. Finkbeiner, D. P. 2004, Astrophys. J., 614, 186
31. Gödel, K. 1949, Rev. Mod. Phys., 21, 447
32. Goobar, A., Amanullah, R., Kulkarni, S. R., et al. 2017, Science, 356, 291
33. Hall, G. S. & MacNay, L. 2005, Classical and Quantum Gravity, 22, 1493
34. Hartwick, F. D. A. 1987, in NATO Advanced Science Institutes (ASI) Series C, Vol. 207, NATO Advanced
     Science Institutes (ASI) Series C, ed. G. Gilmore & B. Carswell, 281–290
35. Hsueh, J.-W., Despali, G., Vegetti, S., et al. 2018, Mon. Not. R. Astron. Soc., 475, 2438
36. Hsueh, J.-W., Fassnacht, C. D., Vegetti, S., et al. 2016, Mon. Not. R. Astron. Soc., 463, L51
37. Hsueh, J.-W., Oldham, L., Spingola, C., et al. 2017, Mon. Not. R. Astron. Soc., 469, 3713
38. Jee, M. J., Hoekstra, H., Mahdavi, A., & Babul, A. 2014, Astrophys. J., 783, 78
39. Karachentsev, I. D. 2012, Astrophysical Bulletin, 67, 123
40. Kent, S. M. 1987, Astron. J., 93, 816
41. Klypin, A., Kravtsov, A. V., Valenzuela, O., & Prada, F. 1999, Astrophys. J., 522, 82
42. Kormendy, J., Drory, N., Bender, R., & Cornell, M. E. 2010, Astrophys. J., 723, 54
43. Li, P. and Lelli, F. and McGaugh, S. S. and Starkman, N. and Schombert, J. M. 2018, arXiv:1811.00553
44. Li, D., Tang, N., Nguyen, H., et al. 2018, Astrophys. J., Suppl. Ser., 235, 1
45. Lindblom, L., Scheel, M. A., Kidder, L. E., et al. 2004, Phys. Rev. D, 69, 124025
46. MacCrann, N., Zuntz, J., Bridle, S., Jain, B., & Becker, M. R. 2015, Mon. Not. R. Astron. Soc., 451, 2877
47. Massey, R., Kitching, T., & Richard, J. 2010, Reports on Progress in Physics, 73, 086901
48. Meurer, G. R., Obreschkow, D., Wong, O. I., et al. 2018, Mon. Not. R. Astron. Soc., 476, 1624
49. Milgrom, M. 1983, Astrophys. J., 270, 365
50. Milosavljević, M., Koda, J., Nagai, D., Nakar, E., & Shapiro, P. R. 2007, Astrophys. J.l, 661, L131
51. Misner, C. W. & Taub, A. H. 1969, Soviet Journal of Experimental and Theoretical Physics, 28, 122
52. Navarro, J. F. & Benz, W. 1991, Astrophys. J., 380, 320
53. Navarro, J. F., Frenk, C. S., & White, S. D. M. 1996, Astrophys. J., 462, 563

54. Navarro, J. F., Frenk, C. S., & White, S. D. M. 1997, Astrophys. J., 490, 493
55. Obukhov, Y. N. & Hehl, F. W. 1996, Acta Phys. Polon., B27, 2685
56. Oh, S.-H., de Blok, W. J. G., Walter, F., Brinks, E., & Kennicutt, Jr., R. C. 2008, Astron. J., 136, 2761
57. Owen, R., Brink, J., Chen, Y., et al. 2011, Physical Review Letters, 106, 151101
58. Pawlowski, M. S., Kroupa, P., & Jerjen, H. 2013, Mon. Not. R. Astron. Soc., 435, 1928
59. Penrose, R. & Rindler, W. 1986, Spinors and Space-time, Volume 2 (Cambridge: Cambridge University Press)
60. Planck Collaboration, Ade, P. A. R., Aghanim, N., et al. 2013, Astron. Astrophys., 554, A139
61. Purcell, C. W., Bullock, J. S., Tollerud, E. J., Rocha, M., & Chakrabarti, S. 2011, Nature, 477, 301
62. Ruiz-Granados, B., Rubino-Martin, J. A., Florido, E., & Battaner, E. 2010, Astrophys. J., 723, L44
63. Saracco, P., Gargiulo, A., & Longhetti, M. 2012, Mon. Not. R. Astron. Soc., 422, 3107
64. Seifert, M. D. 2007, Phys. Rev. D, 76, 064002
65. Shannon, R. M., Ravi, V., Coles, W. A., et al. 2013, Science, 342, 334
66. Snowden, S. L., Egger, R., Freyberg, M. J., et al. 1997, Astrophys. J., 485, 125
67. Su, M., Slatyer, T. R., & Finkbeiner, D. P. 2010, Astrophys. J., 724, 1044
68. Trujillo, I., Carretero, C., & Patiri, S. G. 2006, Astrophys. J., Lett., 640, L111
69. Tumlinson, J., Thom, C., Werk, J. K., et al. 2011, Science, 334, 948
70. Wald, R. 2009, in Workshop on Tests of Gravity and Gravitational Physics, Cleveland, Ohio
71. Wojnar, A., Sporea, C., & Borowiec, A., 2018, Galaxies, 6(3), 70
72. Wu, X.-B., Wang, F., Fan, X., et al. 2015, Nature, 518, 512
73. Xu, D., Sluse, D., Gao, L., et al. 2015, Mon. Not. R. Astron. Soc., 447, 3189
74. Yau, S. T. 1978, Communications on Pure and Applied Mathematics, 31 (3): 339–411
75. Yunes, N. & Siemens, X. 2013, Living Reviews in Relativity, 16, 9
76. Zhang, F., Brink, J., Szilágyi, B., & Lovelace, G. 2012, Phys. Rev. D, 86, 084020
77. Zimmerman, A., Nichols, D. A., & Zhang, F. 2011, Phys. Rev. D, 84, 044037